An experimental investigation of the effect of alkane fuel structure on reactivity demonstrated through the hexane isomers

C. Banyon, K. Zhang, H.J. Curran*

Combustion Chemistry Centre, NUI Galway, Ireland

Abstract

The current work attempts to provide insight into, and improve the fidelity of chemical kinetic models for transportation relevant branched alkanes, which is achieved through a study of the structural isomers of hexane; *n*-hexane, 2-methylpentane, 3-methylpentane, 2,2-dimethylbutane and 2,3-dimethylbutane. The main objectives of this study are to extend the NUIG sub-mechanism to C_6 alkanes, as well as to expand the available species palette for surrogate fuels. To facilitate this study an experimental approach is taken here, while a complementary kinetic modeling study is currently underway. Ignition delay data have been obtained for the five hexane isomers in a high-pressure shock tube (HPST) and in a rapid compression machine (RCM) at $\varphi = 1$, $p = 15$ bar and $X_{O2} = 21\%$ in the temperature range 600–1300 K. At low temperatures (i.e. below 1000 K) the comparative reactivity of the isomers correlates with research octane number, while at high temperatures (i.e. above 1000 K) differences in the ignition delay times between the isomers becomes small. The ignition delay data collected in this study serve as validation targets for the newly developed C_6 mechanism, where good agreement is observed. Future work is planned to use the validated hexane mechanisms to investigate the performance of four- and five-component surrogate mixtures for diesel and gasoline fuels blended with several of the hexane isomers investigated in this study to potentially improve surrogate performance.

Introduction

Advanced combustion strategies that rely on low-temperature, lean-charge, kinetically controlled schemes (e.g. HCCI, RCCI, PPC, etc.) have demonstrated significant progress toward clean, high-efficiency transportation engines [1]. Reliable kinetic models for fuel decomposition and oxidation chemistry facilitate the design of these advanced combustion engines as a predictive tool for assigning ignition timing, rate of heat release, engine-out emissions, etc. While reliable chemical kinetic models for straight-chain alkanes have matured for species relevant to transportation fuels, less work has been conducted on branched alkanes, which can constitute a large fraction of petroleum-derived fuels and their surrogates. Work on branched alkanes has been conducted but very few studies have investigated the influence of alkane isomeric structure on fuel reactivity in the low- to intermediate-temperature regime. Gersen *et al*. [2] and Healy *et al*. [3,4] independently studied the two isomers of butane, *n*- and *iso*-butane, in a rapid compression machine (RCM) over a wide range of conditions. *iso*-Butane was found to be less reactive than *n*-butane, and both fuels showed negative temperature coefficient (NTC) behavior. The three pentane isomers were investigated in an RCM by Ribaucour *et. al*. [5], and more recently by Bugler *et al*. [6]. It was found that *n*-pentane is the most reactive, followed by *neo*-pentane, with *iso*-pentane being the least reactive. The hexane isomers were recently studied by Wang *et al*. [7] in a jet-stirred reactor (JSR) over the low- and intermediate-temperature range. Species concentrations were measured by both gas chromatography and synchrotron vacuum ultraviolet photoionization mass spectrometry. Cyclic ether concentrations were measured for all of the isomers, which are an important intermediate species in the NTC regime. Ignition delay times were measured in an RCM for the nine heptane isomers by Silke *et al*. [8]. It was found that fuel reactivity correlates with the amount of branching in the fuel, where the more branched isomers were less reactive. Fuel reactivity in the NTC region was also found to correlate with research octane number (RON).

The current work attempts to provide insights into, and improve the fidelity of chemical kinetic models for transportation relevant branched alkanes, which is achieved through a study of the structural isomers of hexane; *n*-hexane (nH), 2-methylpentane (2MP), 3-methylpentane (3MP), 2,2-dimethylbutane (22DMB)

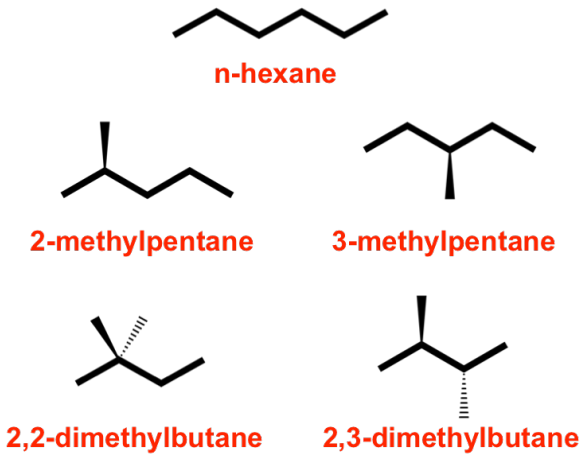

Figure 1 – Chemical structures of the five hexane isomers.

*Corresponding author: henry.curran@nuigalway.ie

and 2,3-dimethylbutane (23DMB). The structures of these five isomers are shown in Fig. 1. The main objective of this study is to provide previously unmeasured ignition delay times for the five isomers of hexane, where this data will be used to validate a new C_6 mechanism, which is currently being developed in a complimentary study [9]. Herein, ignition delay data has been obtained for each of the five hexane isomers in a high-pressure shock tube (HPST) and in an RCM at $\varphi = 1$, $p = 15$ bar and $X_{O2} = 21\%$ in the temperature range 600–1300 K. The HPST facility has been used to measure ignition delays at shorter times ($\tau < 5$ ms), while the RCM is utilized to measure ignition delays at longer times ($\tau > 2$ ms). Within the remainder of this paper a description of the experimental methods utilized is given. After this, the framework used to construct the new C_6 kinetic model is presented, details of which are provided in ref. [9]. Finally, the new ignition data are presented and compared to preliminary predictions of the C_6 mechanisms.

Shock Tube

High-temperature ignition delay times were measured for each of the isomers in the NUIG high-pressure shock tube. The shock tube has previously been described by Nakamura *et al*. [10], however a brief description is also presented here. The 63.5 mm bore tube is comprised of 3 m driver section and a 5.73 m driven section, which are separated by a 3 cm diaphragm section. A double-diaphragm bursting mechanism that utilizes pre-scored, aluminium diaphragms is employed to reach high-pressure reflected shock conditions. Typically, a thin downstream diaphragm is used to promote an ideal bursting and minimize undesirable fluid dynamics during shock formation. The shock velocity is interpolated at five locations along the driven section to account for shock attenuation by measuring the incident shock arrival times at six axially staggered, sidewall mounted PCB 113B24 pressure transducers. The endwall shock velocity is calculated by linearly extrapolating the five velocities to the endwall. Pressure-time histories at the shock tube endwall are monitored using a Kistler 603B pressure transducer mounted flush with the endwall. All pressure signals are recorded using two Handyscope HS4-50 digital oscilloscopes sampling each signal at 5 MHz with 12-bit resolution.

Ignition delay times are measured via the endwall pressure transducer, and are taken to be the time difference between the arrival of the shock wave at the endwall and the arrival of the Von Neumann spike due to ignition, as illustrated in Fig. 2. Well-defined ignition events have been observed for all conditions investigated here.

Herein, test gas temperatures behind the reflected shock were varied by varying the shock velocity, which was achieved by doping the helium driver gas ($P_{4,tot} = 38$ bar) with 0–20% nitrogen. For experiments that resulted in long ignition times (i.e. greater than 1 ms), the total driver gas pressure and nitrogen fraction were simultaneously varied to achieve a tailored interface. For each condition in this study the pressure behind the reflected shock wave was constant at 15 bar to within 10% by adjusting the initial test gas pressures.

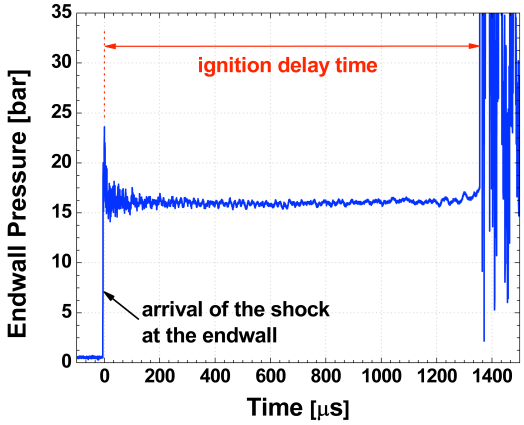

Figure 2 – An example HPST endwall pressure trace, for stoichiometric 3-methylpentane in air at a reflected shock temperature of 1045 K.

The test gas temperature and pressure behind the reflected shock wave are calculated from the endwall shock velocity by solving the 1-D Euler equations with Rankine-Hugoniot jump conditions across the shock. Species thermochemistry are consistent with those used to develop the kinetic model. A description of the methodology used to estimate thermochemistry is presented in ref. [9]. Interactions between the shock wave and boundary layer gases, which lead to a characteristic constant rate of pressure rise, were small for the conditions investigated here. Since, for this study, nearly constant temperature and pressure conditions are maintained behind the reflected shock, adequate comparisons of experimental results and kinetic mechanisms are achieved by utilizing constant volume homogenous reactor models (HRMs) at reflected shock conditions.

The test fuels nH (96%), 2MP (98%), 3MP (99%), 22DMB (97%) and 23DMB (99%) were supplied by TCI UK, and used without further purification. Nitrogen (99.95%) and Oxygen (99.5%) gases were supplied by BOC Ireland. Fuel, oxygen and diluent mixtures were prepared in an external stainless steel mixing vessel fitted with a stirring mechanism. Mixtures were prepared by partial pressure, where liquid fuels are injected and the tank is heated to promote vaporization. The driven section of the shock tube was also heated to prevent fuel condensation prior to an experiment. Mixtures were allowed to homogenize for 20 minutes with active stirring before experiments were conducted.

Rapid Compression Machine

Low- and intermediate-temperature ignition delay times were measured in the NUIG rapid compression machine. This is a clone of the RCM originally built by Affleck and Thomas [11], and has more recently been described by Brett *et al*. [12]. However, a brief

description is provided here. In this device, two opposed pistons volumetrically compress a fuel mixture in about 16 ms to create and maintain a high temperature and pressure environment. At the end of the stroke the pistons are locked, allowing a constant volume reaction to proceed. The pistons are pneumatically driven and locked, while a chamber filled with hydraulic oil along the connecting rod is used to actuate the pistons and control their trajectory. The machine has a 168 mm stroke and 38.2 mm bore. The fuel mixture pressure-time history is recorded in the reaction chamber by a Kistler 601A pressure transducer mounted in the sidewall of the machine. The position of the pistons are monitored by a Positek P100 linear inductive position sensor which is inserted into the machine's hollow connecting rod. The pressure transducer signal is amplified by a Kistler 5018 unit. All signals are recorded by a PiscoScope 4424 digital oscilloscope at 50 MHz with 8-bit resolution. The reaction chamber pressure signal is then smoothed during post-processing by employing a digital low-pass filter with a cut-off frequency of 2.7 kHz.

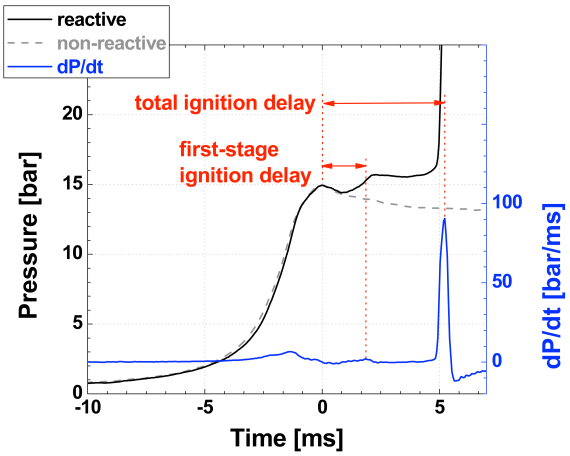

Figure 3 – An example RCM pressure trace for stoichiometric 2-methylpentane in air at a compressed temperature of 733 K.

Ignition delay times are measured from the reaction chamber pressure-time histories, which are taken as the time between the end of compression and the maximum rate of pressure rise due to the main chemical heat release, as illustrated in Fig. 3. A steep pressure rise is observed for all ignition events investigated here.

In this study, compressed gas temperatures were varied in two ways. In the first method the temperature of the reaction chamber surfaces are adjusted via an electrical heating system around the reaction chamber. Great care has been taken to reduce thermal stratification within the reaction chamber. The reaction chamber is heated to a maximum temperature of 120 ^{o}C to avoid degradation of mechanical seals within the machine. For access to temperature regimes outside of the preheating limits the diluent gas composition is varied. For this study, experiments were conducted in a pure nitrogen diluent, a 0.65 Ar : 0.35 N_2 diluent, and a 0.65 CO_2 : 0.35 N_2 diluent for the temperature ranges of 700–820 K, 820–1000 K and 600–700 K, respectively. The compressed pressure was held at 15 bar within 1% for all of the experiments presented here by adjusting the initial fuel mixture fill pressure.

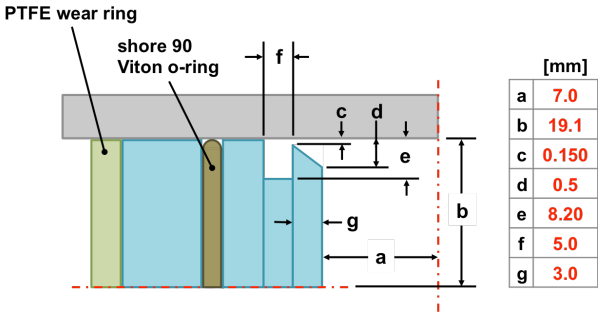

Figure 4 – Schematic of the RCM piston head geometry.

The RCM employs creviced piston heads, as illustrated in Fig. 4, which have been shown through several experimental and computational studies to suppress the formation of in-cylinder roll-up vortices within the boundary layer gases. The suppression of these vortices significantly reduces in-cylinder in-homogeneities. The current geometry of the pistons are a modified design of the optimum that is suggested by Würmel *et al.* [13], which is shown in Fig. 4. These were designed with a large crevice volume to extend the RCM to low-pressure, and high-argon concentration conditions.

While the geometrically optimized creviced pistons minimize advective heat transfer from the cool boundary layer gases into the fuel charge, enthalpic losses from the test gases to the piston crevice volumes as well as diffusive heat flux from the hot charge to the cool reaction chamber walls must be accounted for to make suitable comparisons between experimental RCM data and chemical kinetic models. This is achieved here by employing a two-zone model for the in-cylinder gases, where one zone contains the small volume of inhomogeneous, non-reactive boundary layer gases while the other contains the homogenous, reactive "adiabatic core" gases. Mechanical equilibrium is assumed between the two zones, and the HRM temperature is obtained by isentropically compressing or expanding the "adiabatic core" volume at a rate derived from the experimentally measured pressure history. However, to isolate the effects of transport processes from chemical heat release in the measured pressure histories it is necessary to compress a non-reactive mixture at each experimental condition with matched transport properties of the reactive mixture; an example is shown in Fig. 3. In this study, "adiabatic core" expansion rates are determined at each experimental condition by compressing an additional fuel mixture, where the oxygen fraction is replaced with nitrogen.

Mixtures were prepared in the same manner as described for the HPST, however active stirring was not

available in the mixing vessels. Therefore, test mixtures were allowed to diffusively mix for 12 hours before experiments were conducted. In addition to the fuels and gases described in the HPST section argon (99.95%) and carbon dioxide (99.5%), supplied by BOC Ireland, were also used.

Kinetic Mechanism Development

A kinetic modeling study, which is complementary to the work shown here, for the hexane isomers is currently underway at NUIG. The details of the newly developed C_6 mechanism are provided in ref. [9], however a very brief description is given here.

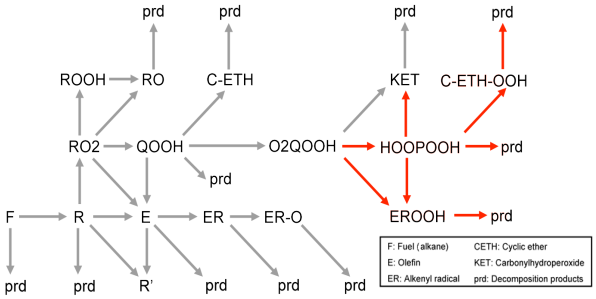

Figure 5 – A schematic of the reaction pathways considered for the hexane isomers.

The C_6 mechanism is built on top of the extensively validated AramcoMech1.3 mechanism [14]. A very recently developed sub-mechanism for the pentane isomers is also included [15]. The framework of the C_6 mechanism considers conventional alkane reaction classes, and also considers the alternative low-temperature pathways shown in Fig 5. While rate constants calculated at a high level of theory or derived from experiments are abundant for smaller species (i.e. C_5 or smaller), few rate constants for larger species are available. Due to the lack of literature rate constants for many of the C_6 mechanism reactions, estimations from modern rate rules and analogies are utilized for many of the rate constants in this work. Species thermochemistry is determined using group additivity, where updated group values from quantum chemical calculations, experiments and online databases have been employed.

Results

The experimental and modeling results for the hexane isomers are shown in Fig. 6. This Arrhenius plot displays the RCM data (closed symbols) and HPST data (open symbols) against simulation results of the new C_6 mechanism (lines) for the five isomers of hexane; nH, 2MP, 3MP, 22DMB and 23DMB. In Fig. 6, the compressed temperature for HPST data is assigned as the test mixture temperature behind the reflected shock, and the compressed temperature is defined as the end of stroke test gas temperature for RCM experiments.

From inspection of Fig. 6, a non-smooth transition from ignition delay times as a function of temperature

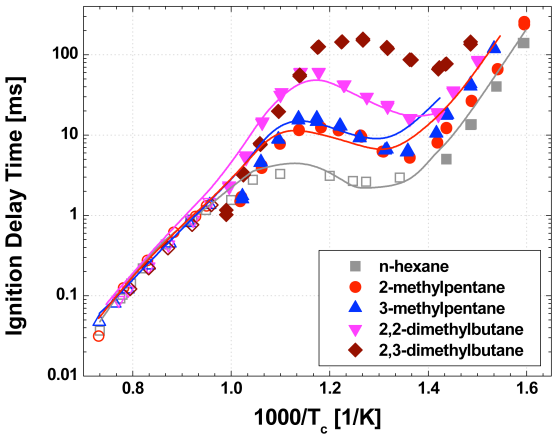

Figure 6 – Ignition delay and modeling results for the hexane isomers, for stoichiometric fuel mixtures in air at a compressed pressure of 15 bar. Open symbols represent HPST data, closed symbols represent RCM data, and lines represent kinetic modeling results.

obtained in the HPST to RCM is observed. This inconsistency is characteristic of comparing shock tube and RCM results, and is due to non-ideal effects during RCM experiments. For instance, at more reactive conditions (i.e. ignition times of less than ~5 ms) the test gas residence time at elevated temperatures during piston compression becomes long compared to chemical time scales, and this effect shortens ignition times when defined from the end of the stroke. At less reactive RCM conditions (i.e. above ~5 ms) heat losses from the test gases to the reaction chamber walls protract ignition delay times. While the non-ideal effects of the RCM facility make direct experimental comparisons between ignition times obtained in the RCM and HPST difficult, sound comparisons can be made between the kinetic mechanism and both facilities by accounting for the transport process in RCM experiments as described in the previous section.

An overall good agreement is observed between the kinetic model for nH, 2MP, 3MP and 22DMB and the HPST and RCM ignition delay times. The model for 23DMB is currently in progress and the preliminary results are not shown here. The performance of the mechanisms at high temperatures and within the NTC is excellent, while the models slightly over-predict the low temperature ignition delay times for all of the isomers. It is beyond the scope of the current study to offer possible explanations for this disagreement, with a more rigorous analysis detailed in ref. [9].

In this study, the experimentally observed low-temperature (i.e. below 1000 K) reactivity for the hexane isomers follows trends consistent with the

Table 1 – Research octane number (RON) and motored octane number (MON) for the isomers of hexane. These values have been tabulated from ref. [16].

Species	nH	2MP	3MP	22DMB	23DMB
RON	24.8	73.4	74.5	91.8	104.3
MON	26.0	73.5	73.3	93.4	94.2

research octane number (RON), which is encouraging and strengthens confidence in the RCM data presented here.

The RON and motored octane number (MON) value for each of the isomers is presented in Table 1 from increasing resistance to autoignition (i.e. decreasing reactivity), which also corresponds to increasing fuel structure branching. The same reactivity hierarchy for the isomers is most drastically observed in this study within the NTC region, where fuel reactivity decreases with increasing temperatures.

One interesting trend in comparative reactivity between 22DMB and 23DMB should be noted for the low-temperature data collected here. At temperatures slightly higher than the NTC region (i.e. 850–1000 K) a cross over is observed in the reactivity of 22DMB and 23DMB, where 23DMB ignites faster than 22DMB. This crossover correlates with MON for 22DMB and 23DMB, where the MON of both fuels are virtually identical. Motored octane number is determined at an engine speed of 900 rpm and an intake temperature of 149 ^{o}C, and RON is determined at an engine speed of 600 rpm and an intake temperature of 52 ^{o}C [17]. The higher engine intake temperature during the MON test leads to higher combustion temperatures. So it is expected that we see a region in the RCM data that correlates with RON, and then a region at slightly elevated temperature that correlates with MON.

The relative increase in reactivity of 23DMB is hypothesized to occur due to the higher available sites where the concerted elimination of hydroperoxyl radicals can occur after molecular oxygen addition to the fuel radical. The rapid production of hydroperoxyl radicals lead to a higher rate of production of hydrogen peroxide in 23DMB after hydrogen abstraction by HO_2 radicals. At the temperatures where crossover occurs the high barrier for hydrogen peroxide decomposition into hydroxyl radicals is overcome and fuel reactivity of 23DMB is promoted more than 22DMB. A more rigorous analysis of the new kinetic mechanisms is required to confirm this hypothesis.

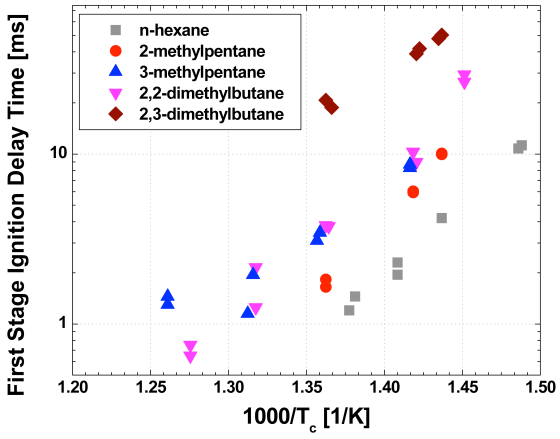

Figure 7 – First stage ignition collected in the RCM for stoichiometric fuel mixtures in air at a compressed pressure of 15 bar.

The experimentally observed high-temperature (i.e. above 1000 K) ignition times of the hexane isomers are very similar. Further analysis of the new kinetic mechanism is needed to explain the small difference in reactivity between the isomers at high temperature.

The first stage ignition delay times have been measured in the RCM for each of the isomers. As was previously observed with the hot ignition event, the first stage ignitions for the isomers follow trends in RON. However, the first stage ignition delay times for 3MP and 22DMB are very similar; the reason for this phenomenon is presently unclear.

Summary

In this study the reactivity of the five isomers of hexane were compared. This was achieved through an experimental approach where ignition delay times for *n*-hexane, 2-methylpentane, 3-methylpentane, 2,2-dimethylbutane and 2,3-dimethylbutane were measured in a high-pressure shock tube and rapid compression machine at φ = 1, p = 15 bar and X_{O2} = 21% in the temperature range 600–1300 K. Low- and intermediate-temperature fuel reactivity was found to correlate with the amount branching within the fuel, where *n*-hexane was found to be the most reactive, followed by 2-methylpentane and 3-methylpentane, followed by 2,2-dimethylbutane and finally followed by the least reactive 2,3-dimethylbutane. Comparative ignition delay times correlated with research octane number in the NTC region, while the reactivity of the isomers became very similar above 1000 K. A new kinetic oxidation mechanism for the hexane isomers was compared against the ignition delay data, and an overall satisfactory performance of the model was observed.

Future work is planned to provide a more rigorous validation of the new C_6 mechanism against the speciation data of Wang *et al.* [7]. Also, work is planned to evaluate the potential of the hexane isomers as real-fuel surrogates.

Acknowledgements

The research leading to these results has received funding from the People Programme (Marie Curie Actions) of the European Union's Seventh Framework Programme FP7/2007-2013/ under REA grant agreement no 607214.

References

[1] R. D. Reitz, G. Duraisamy, Prog. Energ. Combust. 46:12-71 (2015).

[2] S. Gersen, A. V. Mokhov, J. H. Darmeveil, H. B. Levinsky, Combust. Flame 157:240-245 (2010).

[3] D. Healy, N. S. Donato, C. J. Aul, E. L. Petersen, C. M. Zinner, G. Bourque, H. J. Curran, Combust. Flame 157:1526-1539 (2010).

[4] D. Healy, N. S. Donato, C. J. Aul, E. L. Petersen, C. M. Zinner, G. Bourque, H. J. Curran, Combust. Flame 157:1540-1551 (2010).

[5] M. Ribaucour, R. Minetti, L. R. Sochet, H. J. Curran, W. J. Pitz, and C. K. Westbrook, P. Combust. Inst. 28:1671-1678 (2000).
[6] J. Bugler, B. Marks, O. Mathieu, R. Archuleta, K. A. Heufer, E. L. Petersen, H. J. Curran, (2015) (submitted for publication).
[7] Z. Wang, O. Herbinet, Z. Cheng, B. Husson, R. Fournet, F. Qi, F. Battin-Leclerc, J. Phys. Chem. A 118:5573–5594 (2014).
[8] E. J. Silke, H. J. Curran, J. M. Simmie, Proc. Combust. Inst. 30:2639-2647 (2005).
[9] K. Zhang, C. Banyon, J. Bugler, H. J. Curran, A kinetic modeling study on the oxidation of five hexane isomers, Proceedings of the 7th European Combustion Meeting, Budapest, Hungary (2015).
[10] H. Nakamura, D. Darcy, M. Mehl, C.J. Tobin, W.K. Metcalfe, W.J. Pitz, C.K. Westbrook, H.J. Curran, Combust. Flame 161:49-64 (2014).
[11] Affleck, W. S., and Thomas, A., Proc. Inst. Mech. Eng. 183:365–385 (1969).
[12] L. Brett, J. Macnamara, P. Musch, J. M. Simmie, Combust. Flame 124:326-329 (2001).
[13] J. Würmel and J. M. Simmie, Combust. Flame 141:417-430 (2005).
[14] W. K. Metcalfe, S. M. Burke, S. S. Ahmed, H. J. Curran, Int. J. Chem. Kinet. 45: 638–675 (2013).
[15] J. Bugler, K. P. Somers, E. J. Silke, H. J. Curran, (2015) (submitted for publication).
[16] Phillips 66 Reference Data for Hydrocarbons and Petro-Sulfur Compounds, Bulletin No. 521, Phillips Petroleum Company, 1962 (revised 1974).
[17] J. B. Heywood, Internal Combustion Engine Fundamentals, McGraw-Hill, 1988.